Inverse photoemission from electronic surface states: Intensity, angular, and polarization dependence

Trninić-Radja, B.; Šunjić, Marijan

Source / Izvornik: **Physical Review B (Condensed Matter), 1990, 42, 7409 - 7415**

Journal article, Published version
Rad u časopisu, Objavljena verzija rada (izdavačev PDF)

https://doi.org/10.1103/PhysRevB.42.7409

Permanent link / Trajna poveznica: https://urn.nsk.hr/urn:nbn:hr:217:009549

Rights / Prava: In copyright / Zaštićeno autorskim pravom.

Download date / Datum preuzimanja: **2025-03-13**

Repository / Repozitorij:

Repository of the Faculty of Science - University of Zagreb

Inverse photoemission from electronic surface states: Intensity, angular, and polarization dependence

B. Trninić-Radja*
Department of Physics, University of Zagreb, P.O. Box 162, YU-41001 Zagreb, Croatia, Yugoslavia

M. Šunjić
International Centre for Theoretical Physics, strada Costiera 11, Miramire, P.O. Box 586, I-34100, Trieste, Italy and Department of Physics, University of Zagreb, P.O. Box 162, YU-41001 Zagreb, Croatia, Yugoslavia†

(Received 10 October 1989; revised manuscript received 31 January 1990)

The independent-particle model of inverse photoemission is defined and applied to study the properties of emitted-photon spectra in a system that can be treated analytically: electronic (image-potential) states on dielectric-covered metal surfaces. In particular, analytic expressions for the matrix elements are evaluated, and the intensity, angular, and polarization dependence are discussed.

I. INTRODUCTION

Inverse-photoemission spectroscopy (IPES) or bremstrahlung isochromat spectroscopy (BIS) is fast becoming a standard method for investigating unoccupied electronic states in solids, especially at surfaces.[1–5] One of the interesting examples is the study of image-potential- and crystal-induced states on clean and dielectric-covered metal surfaces[1,6–8] where angle-resolved (or k-resolved) IPES has already provided much essential information,[1,4,9] as a technique complementary to low-energy electron diffraction (LEED) (Ref. 10) and electron-energy-loss spectroscopy (EELS) (Ref. 11) investigations of these states.

In spite of enormous recent experimental activity in this field,[1–9] there was much less theoretical work on IPES. Omitting earlier BIS calculations which deal with phenomena at higher electron and photon energies (and therefore explore mostly the atomiclike levels in the bulk), only a few papers treated IPES theoretically.[12–14] Pendry[13] used his previous experience with LEED in a way similar to his formulation of uv photoemission theory,[15] to write the photon current in inverse photoemission (IP) with matrix elements which contain the LEED wave functions for the incoming electron. The theory is essentially a single-particle theory, because the inelastic effects are treated using the optical-potential and mean-free-path approximations. However, strong multiple-scattering effects in this system require numerically calculated wave functions and matrix elements, which prevent a detailed qualitative discussion of the properties of IP spectra.[13(a)] Johnson and Davenport[14] developed the expression for the IP differential cross section from atomic or molecular levels of adsorbates, in line with earlier work[16] on photoemission from single oriented molecules.

In this paper we first define the independent-particle approximation of IPES and indicate the approximations made in its derivation from a full many-body formulation (Sec. II). In Sec. III we apply it to IPES from two-dimensional electronic states localized at surfaces, and discuss general properties of the photon spectra—angular, polarization, and energy dependence. We briefly introduce the image-potential states on dielectric-covered metal surfaces. Using the analytic wave functions of this model system we calculate the matrix elements which give the intensities of emitted radiation. In Sec. IV we discuss the angular dependence and intensities of emitted radiation.

II. INDEPENDENT-PARTICLE APPROXIMATION OF THE INVERSE-PHOTOEMISSION SPECTRUM

In inverse photoemission an electron with momentum $\mathbf{k}$ and energy $E_{\mathbf{k}}$ is impinging at an angle ϑ on a semifinite sample, and photons with fixed energy $\hbar\omega_{\mathbf{q}}$ (momentum $\mathbf{q}$) are observed.

For the transition $|\mathbf{k}\rangle \rightarrow |\tilde{\lambda}\rangle$ into the bound state $|\tilde{\lambda}\rangle$ with emission of photons with wave vector $\mathbf{q}$, polarization $\epsilon_{\mathbf{q}}$, and frequency $\omega \equiv \omega_{\mathbf{q}}$, the differential cross section in the dipole approximation is

$$\frac{d\sigma(\omega)}{d\Omega} = \frac{\alpha}{2\pi}\frac{\omega}{mc^2}\frac{V_e}{\hbar k\cos\vartheta}|\langle \mathbf{k}|\epsilon_{\mathbf{q}}\cdot\mathbf{p}|\tilde{\lambda}\rangle|^2 , \qquad (2.1)$$

where the fine-structure constant $\alpha = e^2/\hbar c \approx \frac{1}{137}$, $\mathbf{p}$ is the electron momentum operator, and V_e is the electron normalization volume.

In principle, in order to describe completely the inverse photoemission spectrum one would require a full many-body formulation. In analogy with the steps and the discussion in the photoemission case,[17] one can[18] reduce the full many-body result for the inverse photoemission spectrum to the independent-particle approximation (2.1). Here we shall just briefly mention these assumptions.

(1) In the "sudden approximation," we neglect the interaction of the incoming electron with the solid. The justification for this approximation in PE is usually based

 ©1990 The American Physical Society

on the high photoelectron velocity which reduces scattering probabilities. In IPES, for the energies we are considering, the situation is different: electron energies are below threshold for many discrete excitation mechanisms (e.g., plasmons or ionization losses). However, one cannot exclude the low-energy excitations (electron-hole pairs, phonons) but one expects that they will give small and/or smooth background in the spectra. Thus we have neglected all "extrinsic" (inelastic) scattering, and the IPE spectrum reduces to that of the final electron state $\tilde{\lambda}$.

(2) We also neglect "intrinsic" inelastic effects, i.e., the satellites due to the scattering in the final state $\tilde{\lambda}$. This means that the cross section (2.1) describes only the elastic (no-loss) peak in the spectrum. This approximation is good for weak scattering, but it may overestimate the no-loss intensity, because in principle it violates the spectral sum rule.[18]

(3) The final state contains one photon $\mathbf{q}$ and $N+1$ interacting particles (i.e., one extra electron in the state λ, filled by the transition from $|\mathbf{k}\rangle$). The addition of an electron will lead to relaxation due to its interaction with other N particles and their degrees of freedom in the system, and to the lowering of its energy $E_\lambda \rightarrow \tilde{E}_\lambda$ with respect to the noninteracting system. This relaxation shift of the final state shall be neglected in our case because of two arguments: the state is spread out, i.e., delocalized in two dimensions, and it is rather close to the Fermi level.[18] For all these reasons, in the following we shall use the independent-particle approximation (2.1).

III. INVERSE PHOTOEMISSION FROM ELECTRONIC SURFACE STATES

Here we shall study inverse photoemission from electronic states localized at surfaces, in particular the image-potential states.[19] In the independent-particle approximation the final bound electron state $|\tilde{\lambda}\rangle$ is the solution of the Schrödinger equation in the surface potential which is dominated by the repulsive potentials of the surface atomic cores, and the electrostatic (attractive) image-like potential. Due to translational symmetry parallel to the surface, the electronic initial- and final-state wave functions factorize

$$\Psi_{\mathbf{k}}(\mathbf{r}) = V_e^{-1/2} e^{iK\cdot\rho}|\kappa\rangle; \quad \Psi_{\mathbf{K}\nu}(\mathbf{r}) = A^{-1/2} e^{iK\cdot\rho}|\nu\rangle \ . \tag{3.1}$$

$|\kappa\rangle$ describes the incoming electron elastically scattered at the surface [see Fig. 1(a)]. As a reasonable approximation, valid outside the short range of the atomic core potentials, we shall later use a reflected plane wave (RPW):[20]

$$|\kappa\rangle = e^{-i\kappa(z-\Delta)} + R(E,\Omega)e^{2i\delta(E,\Omega)}e^{i\kappa(z-\Delta)} \ . \tag{3.2}$$

Here, $R(E,\Omega)$ gives the LEED reflectivity and $\delta(E,\Omega)$ is the scattering phase shift. $|\nu\rangle$ is the wave function of the surface state, to be specified later.

The energy of the final localized state is the sum of the parallel $\hbar^2K^2/2m_\nu^*$ and perpendicular energy $E_\nu < 0$. E_ν is the binding energy with respect to the vacuum level, and m_ν^* is the effective electron mass in the state ν.

Parallel-momentum and total-energy conservation imply that the photon is emitted with the energy

$$\hbar\omega_q = E\cos^2\vartheta + |E_\nu| + E\sin^2\vartheta(1 - m/m_\nu^*) \ . \tag{3.3}$$

Defining the s-or p-polarization vectors in (2.1), and with the photon angles shown in Fig. 1(b), we obtain the emitted-photon intensities in the solid angle between Ω and $\Omega + d\Omega$ per single incoming electron:

$$dI_p(\omega) = \frac{\alpha}{2\pi}\frac{\hbar\omega}{mc^2}\frac{k}{\cos\vartheta} \times [K_0^2\cos^2\theta\cos^2\Phi|M_\parallel|^2 + \kappa_0^2\sin^2\theta|M_\perp|^2 - K_0\kappa_0\sin2\theta\cos\Phi\,\mathrm{Re}(M_\parallel\cdot M_\perp^*)]d\Omega \ , \tag{3.4a}$$

$$dI_s(\omega) = \frac{\alpha}{2\pi}\frac{\hbar\omega}{mc^2}\frac{k}{\cos\vartheta}(K_0^2\sin^2\Phi|M_\parallel|^2)d\Omega \ , \tag{3.4b}$$

where $K_0 \equiv K/k = \sin\vartheta$ and $\kappa_0 \equiv \kappa/k = \cos\vartheta$. The matrix elements are

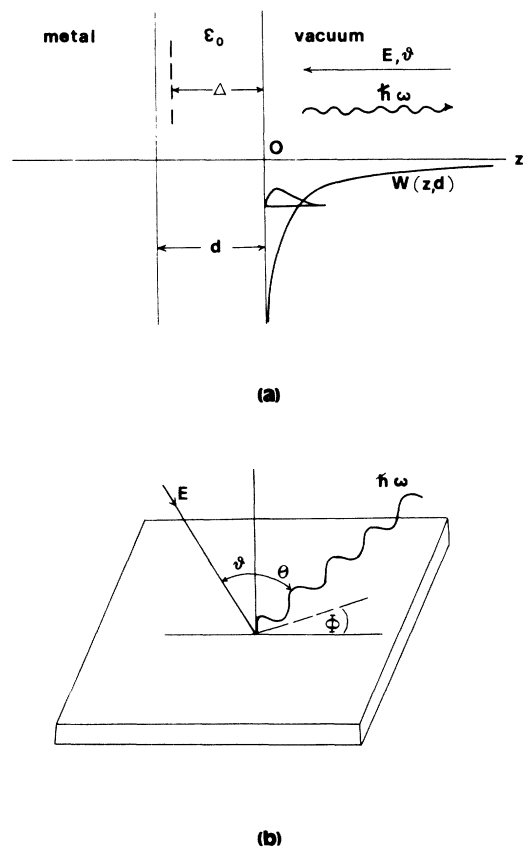

FIG. 1. (a) Energy scheme for electrons trapped in the image potential $W(z,d)$ on a layer of dielectric ($-d < z < 0$) deposited on a metal substrate ($z < -d$). $|R|^2$ is the reflectivity of incoming electrons at the surface, δ is the scattering phase shift, and Δ defines the reflection plane of impinging electrons. (b) Geometry of the system, with incoming electron (ϑ) and emitted photon angles (θ,Φ).

$$M_{\parallel}^{\nu}=\langle\kappa|\nu\rangle,\quad M_{\perp}^{\nu}=\frac{1}{i\kappa}\left\langle\kappa\left|\frac{d}{dz}\right|\nu\right\rangle . \tag{3.5}$$

The cross section (3.4) is normalized to the unit electron current per unit area, to get the number of s- and p-polarized photons emitted per single electron of energy E impinging on the surface. For unpolarized light the total photon intensity is the sum of (3.4a) and (3.4b).

In some experiments the photons are collected in a cone $\theta<\theta_0$, so the total intensity is found by integrating (3.4). That is, the total number of photons emitted into a half-space ($\theta_0=\pi/2$) is

$$I(\omega)=\tfrac{2}{3}\alpha\frac{\hbar\omega}{mc^2}\frac{k}{\cos\vartheta}(K_0^2|M_{\parallel}|^2+\kappa_0^2|M_{\perp}|^2) . \tag{3.6}$$

In order to give and discuss quantitative results for a well-defined problem, possibly obtaining analytical expressions for the matrix elements (3.5), we need some reasonable analytical form for the final-state wave functions (3.1), assuming RPW's (3.2) for the incoming electrons. In Ref. 21 we found variational hydrogeniclike wave functions of image-potential states of electrons trapped on dielectric layers supported by metallic substrates, and checked their accuracy by comparing them with exact numerical results. The eigenstates and eigenenergies were calculated for three inert dielectrics: liquid He and solid Ne and Ar for the three lowest image-potential states, in excellent agreement with full numerical results. With these wave functions the matrix elements (3.5) can easily be evaluated:

$$M_{\perp,\parallel}^{\nu}=\Psi_{\perp,\parallel}^{\kappa,\nu}\pm\mathrm{Re}^{2i(\Delta\kappa-\delta)}\Psi_{\perp,\parallel}^{-\kappa,\nu} , \tag{3.7}$$

where $\Psi^{\kappa,\nu}$ are Fourier transforms of the wave functions:[21]

$$\Psi_{\perp,\parallel}^{\kappa,\nu}=\int_{\Delta}^{\infty}e^{i\kappa(z-\Delta)}\begin{pmatrix}d/dz\\1\end{pmatrix}\Psi_{\nu}(z)dz,\quad \nu=0,1,2 . \tag{3.8}$$

The mean free path in all noble-gas crystals is larger than $220a_0$ for electrons with energies below 10 eV and above the vacuum level.[22] Therefore we might consider absorbate layers to be transparent for incoming electrons in the energy region we are interested in. They can only be reflected on the underlying metal substrate, leading to $\Delta<0$. But the surface-state wave functions are different from zero for $z>0$ [$z=0$ is the boundary of the dielectric; see Fig. 1(a) and Ref. 21] in our barrier model[21] so Δ in (3.8) only contributes a phase factor because integration starts at $z=0$. Then the Fourier transforms (3.7) are

$$\Psi_{\parallel}^{\kappa,\nu}=\Psi_{\perp}^{\kappa,\nu}=\Psi_{\nu}^{\kappa} \tag{3.9}$$

and in particular the following.

(i) The ground state:

$$\Psi_0^{\kappa}=\frac{1}{N_0}\frac{1}{\beta_0^2} .$$

(ii) The first excited state:

$$\Psi_1^{\kappa}=\frac{1}{N_1}\left[\frac{a_1}{\beta_1^2}+\frac{2a_2\alpha_1}{\beta_1^3}\right] .$$

(iii) The second excited state:

$$\Psi_2^{\kappa}=\frac{1}{N_2}\left[\frac{b_1}{\beta_2^2}+\frac{2b_2\alpha_2}{\beta_2^3}+\frac{6b_3\alpha_2^2}{\beta_2^4}\right] ,$$

where

$$\beta_{\nu}=\frac{\alpha_{\nu}}{4(\nu+1)}-i\kappa;\quad N_{\nu}^2=16(\nu+1)^3a_0^3,\quad \nu=0,1,2 .$$

Orthonormalization conditions give five relations which determine coefficients a_i,b_i as functions of the variational parameters α_0, α_1, and α_2 for each dielectric thickness d.[21]

In Sec. IV we shall consider two extreme values for the reflectivity coefficient R in the calculation of matrix elements (3.5). The choice $R=0$ would correspond to the situation where the perpendicular energies of impinging electrons are outside the gap in the projected bulk band structure, as in the case of the Pd(111) surface for the electrons of perpendicular energies ~ 10 eV.[23] For that choice of R,

$$|M_{\parallel}^{\nu}|^2=|M_{\perp}^{\nu}|^2=\mathrm{Re}(M_{\parallel}^{\nu}M_{\perp}^{\nu *}) . \tag{3.10}$$

For impinging electrons with perpendicular energies in the energy gap of the crystal the reflectivity is very high. That is, for Cu(100) and Ni(100) surfaces several eV above vacuum level, the simplest approximation for the surface potential is an infinite barrier, leading to $R=1,\delta=\pi/2$ (top of the energy gap in the Schottky inverted case). The perpendicular and parallel matrix elements are related only for $R=0$. These ideal situations ($R=1$ or $R=0$) assumed in our calculations are quite reasonable approximations for electrons with energies in the middle of the band gap and well away from the gap, respectively, so these cases are of considerable interest for qualitative discussion of intensity and angular distributions of IPES.

IV. DISCUSSION OF THE PHOTON SPECTRA: ANGULAR, POLARIZATION, AND ENERGY DEPENDENCE

From (3.4) it can be seen that electrons at normal incidence give no emitted photons in that direction because

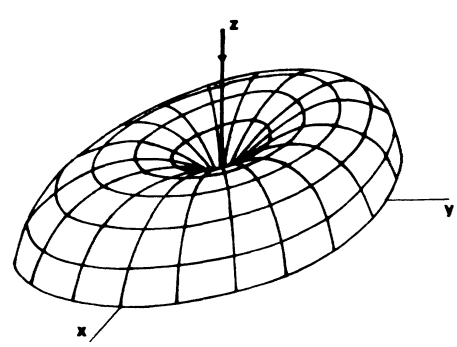

FIG. 2. Angular distribution of p-polarized photons with $\vartheta=0°$.

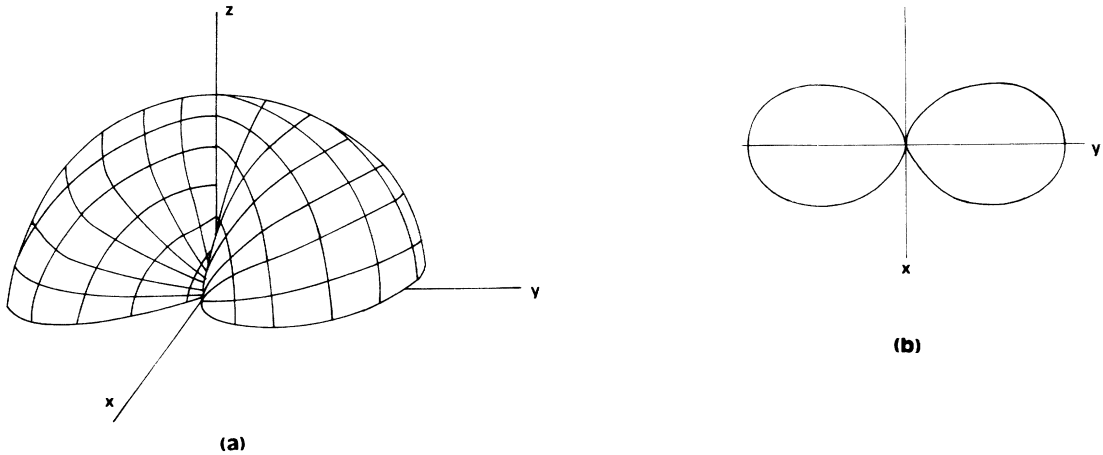

FIG. 3. (a) Angular distribution and (b) cross section with the plane parallel to the surface for s-polarized photons, for any angle ϑ.

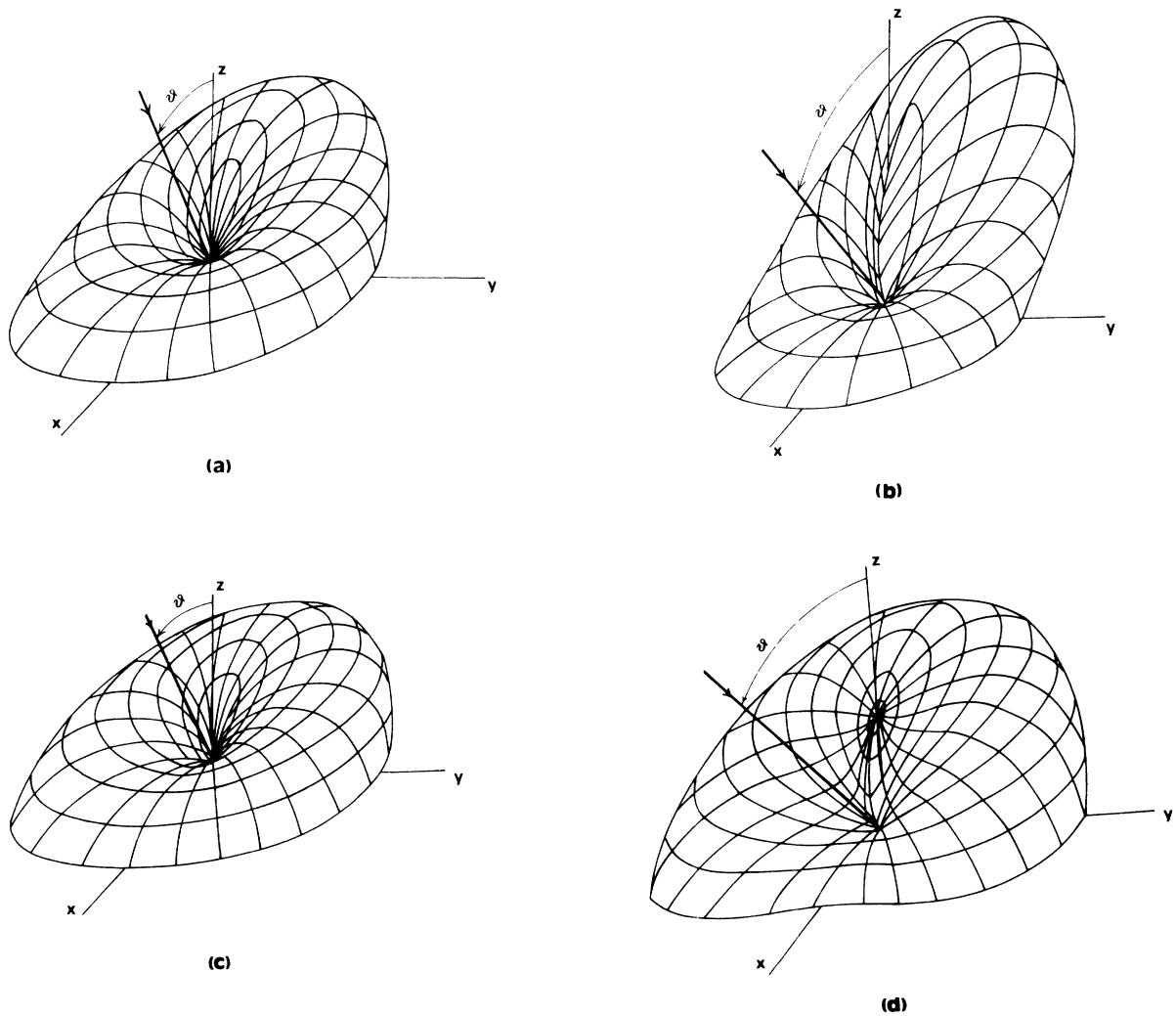

FIG. 4. Angular distribution of p-polarized photons for $R=0$: (a) $\vartheta=25°$, (b) $\vartheta=45°$, and unpolarized photons (c) $\vartheta=25°$, (d) $\vartheta=45°$. The electron directions are indicated.

of simple dipolar matrix elements. For that impinging angle there will be no emission of s-polarized photons, and the intensity of p-polarized photons will be symmetrical with regard to the surface normal (Fig. 2).

In general, the shape of angular distribution will depend on the matrix elements and the electron incident angle. However, the shape of angular distribution of s-polarized photons does not depend on the electron angle, (except for $\vartheta=0°$) the wave function of the incoming electron, or the surface state. Its shape is shown in Fig. 3. The intensity of s-polarized photons in the direction of the incoming electron [see (3.4b)] vanishes. On the other hand, the angular distributions of p-polarized photons and total emitted photons depend on the choice of parameters R, δ, Δ, E, ϑ, and ν, as discussed in the following.

For $R=0$, the shape of angular distribution of p-polarized photons and unpolarized light will be the same for all surface and incoming electron states [see (3.4) and (3.10)], and it will depend only on the direction of the incoming electron (Fig. 4). Only the intensities will change.

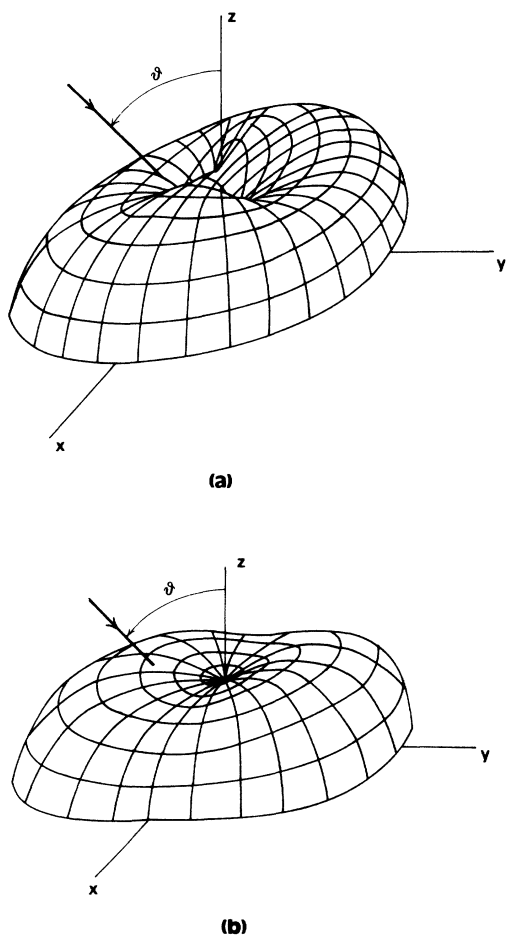

FIG. 5. Angular distribution of (a) p-polarized photons and (b) unpolarized photons, for $\vartheta=45°$, $R=1$, $\delta=\pi/2$, and $d=1a_0$ (Ar on metal). For the $\nu=1$ state and photon energy 9.7 eV, the incoming electron energy is 19 eV.

If $R\neq 0$, it is necessary to take into account the energies and angles of the incoming electrons, as well as the surface state to determine the shape of angular distributions of p-polarized and total emitted photons. In the experiment itself photons of specific energy are detected,

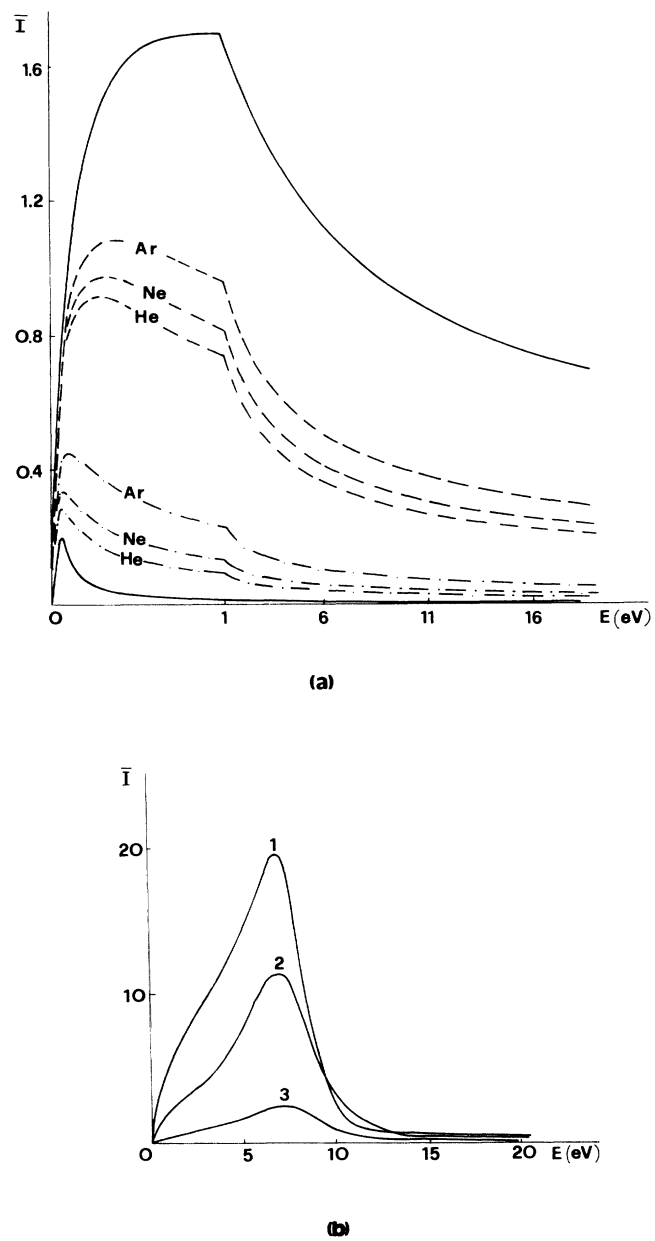

FIG. 6. Intensities of emitted photons $[\bar{I}=I/(9.5\times 10^{-9})]$ as functions of electron energy, for $\vartheta=0°$. (a) For image-potential states in a model with an infinite repulsive wall: solid lines, the ground and first excited surface states on clean metal ($d=0$); dashed (dashed-dotted) lines, the ground state on dielectric-covered metal surface, $d=1a_0$ ($d=10a_0$). (The data are taken from Ref. 21.) (b) For crystal-induced and the first two image-potential states on clean Pd(111) surface. (The wave functions are taken from Ref. 24.)

while the angle and the energy of impinging electrons change. For our discussion of angular distribution of unpolarized light a typical photon energy of 9.7 eV (Ref. 1) can be taken, which automatically fixes the perpendicular energy of impinging electrons if the energy of the surface state is fixed. There is no general rule for the form of p-polarized and unpolarized light. As shown in Figs. 2–5, for $\vartheta=0°$ the intensities are largest at angles close to the surface, and get heavily distorted with tilting electron angle ϑ. This particular feature should be borne in mind in the setting up of the experiment.

In order to estimate the *total intensities,* we examine

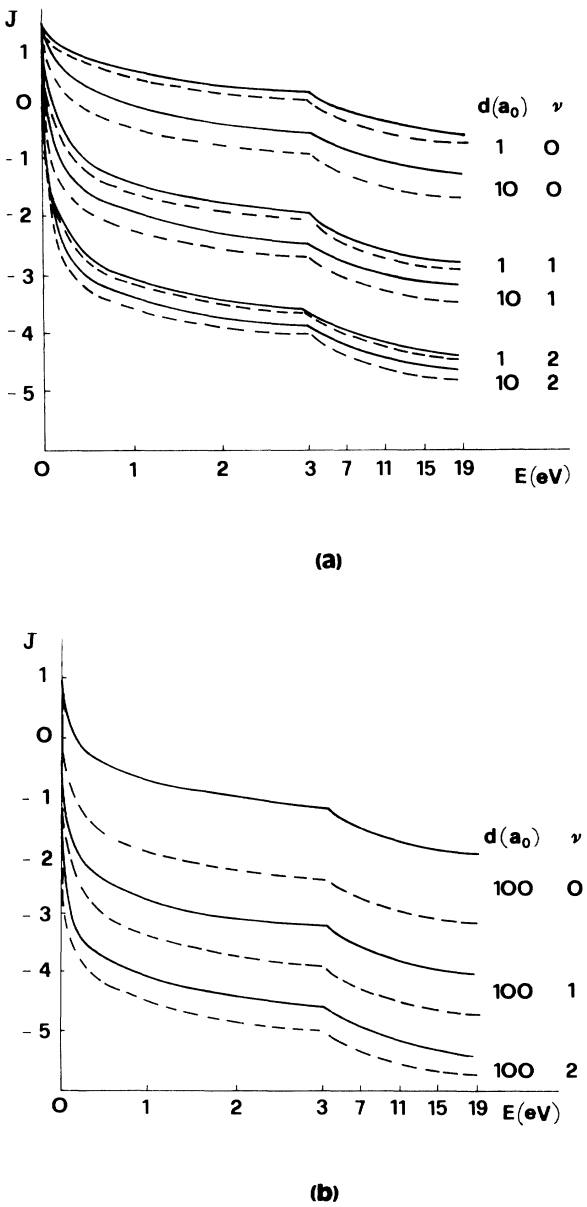

FIG. 7. Dependence of intensity $J \sim \log_{10} I$ on the thickness d of the dielectric layer and on the surface state ν, for $R=0, \vartheta=0°$. (a) Solid lines, Ar ($d=1, 10a_0$); dashed lines, He ($d=1, 10a_0$). (b) Solid lines, Ar ($d=100a_0$); dashed lines, He ($d=100a_0$).

first the case of normal incidence electrons ($\kappa=k$, $\cos\vartheta=1$) and the simplest approximation $R=0$. Then from (3.6) we find that

$$I(\omega)=9.5\times10^{-9}\hbar\omega[\text{eV}]\kappa[a_0^{-1}]\,|M_\perp|^2[a_0]\ . \qquad (4.1)$$

Since the energies of detected photons and perpendicular electron energies are in the region of 10 eV ($\kappa\approx1$ a.u.) the conversion factor, i.e., the number of emitted photons per incoming electron, is of the order of 10^{-7}.

Figure 6(a) shows the photon intensities $\bar{I}\equiv I/(9.5\times10^{-9})$ for the ground and the first excited surface states ($\nu=0,1$) in the potential with an infinite repulsive wall when the dielectric layers (He, Ne, or Ar) of various thicknesses are deposited on metallic substrate, starting with $d=0$. For the broader wave function (higher excited state) the overlap integral $|M_\perp|$ is smaller because the electron wavelength is of the order of 1 Å^{-1}, and accordingly the intensity of emitted photons is lower.

As another model example we can study a clean Pd(111) surface, where the barrier is replaced by a finite gap, so that the electrons can penetrate into the crystal.[24] In this case the intensities for the three lowest surface states (i.e., for $d=0$) increase [Fig. 6(b)]. The data used in the calculation of matrix elements for the Pd(111) surface were taken from Ref. 24. We can see that in the narrow region of electron energies ($\sim$10–13 eV) the intensity of emitted photons is higher when the final state is more strongly bound, and the overlap in matrix elements (3.8) is smaller because of the phase shift between the initial and final electron wave functions. The integration in matrix elements (3.8) in this case goes over the $z<0$ (metal) and $z>0$ (vacuum) regions ($R=0$, and surface-state wave functions penetrate the metal), particularly over the region of constant surface potential where the initial function is a cosine.[24]

This decrease of intensities, dependent on the spatial extent and the excitation energies of surface states, is emphasized in Fig. 7, where the logarithms J of intensities are shown, defined by $J=\log_{10}(\hbar\omega|M_\perp|^2)$ so that $I=9.5\times10^{-9}(10)^J\sqrt{E\ [\text{Ry}]}$.

An increase of the incidence electron angle will result in an increase of intensity. In the case of a plane wave $|M_\perp|^2=|M_\parallel|^2$, so that

$$I(\omega)=9.5\times10^{-9}\hbar\omega[\text{eV}]\frac{\kappa}{\cos^2\vartheta}|M_\perp|^2\ .$$

One cosine factor comes from the fact that in order to keep the perpendicular energy constant (since in the experiment the photons of fixed energy are detected) while increasing the incidence angle, the electron energy has to change simultaneously ($k=\kappa/\cos\vartheta$). The other cosine factor comes from the incoming electron flux, so that the overall conversion factor is increased.

In conclusion, we have presented complete and at the same time relatively simple analytic expressions for the description of IPES from electronic image-potential states in the independent-particle model, and shown general properties of emitted photon spectra. The calculated prefactors give the dependence on the initial and final states of electrons and of emitted photons, and explain

small intensities of emitted radiation in comparison with the PE spectra.

ACKNOWLEDGMENTS

This work was partially supported by the U.S.–Yugoslav Joint Board on Scientific and Technological Cooperation, Grant No. PN-851/NIST. One of us (M.Š.) would like to thank Professor Abdus Salam, The International Atomic Energy Agency and United Nations Educational, Scientific and Cultural Organization (UNESCO) for hospitality at the International Centre for Theoretical Physics, Trieste, and Professor Mario Tosi for the hospitality at the Workshop on Condensed Matter Physics.

*Present and permanent address: Faculty of Mining, Geology, and Petroleum Engineering, University of Zagreb, P.O. Box 186, YU-41001 Zagreb, Croatia, Yugoslavia.

†Permanent address.

[1]V. Dose, Surf. Sci. Rep. **5**, 337 (1985).

[2]P. D. Johnson and S. L. Hulbert, Phys. Rev. B **35**, 9427 (1987).

[3]P. D. Johnson, D. A. Wesner, J. W. Davenport, and N. V. Smith, unpublished.

[4]V. Dose, J. Vac. Sci. Technol. A **5**, 2032 (1987), and references therein.

[5]F. J. Himpsel, J. Phys. Chem. Solids **49**, 3 (1988).

[6]N. V. Smith and D. P. Woodruff, Prog. Surf. Sci. **21**, 295 (1986).

[7]K. Wandelt, W. Jacob, N. Memmel, and V. Dose, Phys. Rev. Lett. **57**, 1643 (1986).

[8]K. Horn, K. H. Frank, J. A. Wilder, and B. Reihl, Phys. Rev. Lett. **8**, 1064 (1986).

[9]D. Straub and F. J. Himpsel, Phys. Rev. B **33**, 2256 (1986).

[10]R. Feder and J. B. Pendry, Solid State Commun. **26**, 519 (1978).

[11]J. E. Demuth, B. N. J. Persson, and A. J. Schell-Sorokin, Phys. Rev. Lett. **51**, 2214 (1983).

[12]G. Borstel and G. Thörner, Surf. Sci. Rep. **8**, 1 (1987).

[13]J. B. Pendry, J. Phys. C **14**, 1381 (1981). (a) For example, Eq. (29) of Ref. 13 might lead to a wrong conclusion that the current is proportional to ω^2 (where $\hbar\omega$ is the photon energy); in fact, the factor hidden in the matrix element should give a correct $\omega\sqrt{E}$ dependence (where E is the energy of the incoming electron in the range 0–20 eV).

[14]P. D. Johnson and J. W. Davenport, Phys. Rev. B **31**, 7521 (1985).

[15]J. B. Pendry, Surf. Sci. **57**, 679 (1976).

[16]J. W. Davenport, Phys. Rev. Lett. **36**, 945 (1976).

[17]M. Šunjić, Phys. Scr. **21**, 561 (1980).

[18]For details, see M. Šunjić and B. Trninić-Radja (unpublished).

[19]Dose, and the references cited therein.

[20]See, e.g., C. B. Duke, Adv. Chem. Phys. **27**, 1 (1974).

[21]B. Trninić-Radja, M. Šunjić, and Z. Lenac, Phys. Rev. B **40**, 9600 (1989).

[22]N. Schwentner, E.-E. Koch, and J. Jortner, *Electronic Excitations in Condensed Rare Gases* (Springer-Verlag, Berlin, 1985), Chap. 7.

[23]N. E. Christensen, Phys. Rev. B **14**, 3446 (1976).

[24]Z. Lenac, M. Šunjić, H. Conrad, and M. E. Kordesch, Phys. Rev. B **36**, 9500 (1987).